J Mater Sci (2008) 43:6049–6056
DOI 10.1007/s10853-008-2959-5

AC conduction in amorphous thin films of SnO_2

M. Anwar · I. M. Ghauri · S. A. Siddiqi

Received: 8 May 2008 / Accepted: 18 August 2008 / Published online: 4 September 2008

Abstract Alternating current (a.c.) electrical properties of thermally evaporated amorphous thin films of SnO_2 sandwiched between aluminium electrodes have been investigated for temperature during electrical measurements, film thickness, substrate temperature and post-deposition annealing. The a.c. conductivity, $\sigma(\omega)$, is found to vary with frequency according to the relation $\sigma(\omega) \propto \omega^s$, indicating a hopping process at low temperature. The conduction is explained by single polaron hopping process as proposed by Elliott. The increase in electrical conductivity with increase in temperature during electrical measurements is ascribed to the increase in the formation and high mobility of doubly ionized oxygen vacancies. The increase in conductivity with increase in film thickness is caused by the increase in interstitial tin, oxygen vacancies and defects produced due to deviation from stoichiometry. The increase in conductivity with increase in substrate and annealing temperature may be due to the formation of singly or doubly ionized oxygen vacancies and tin species of lower oxidation state. Measurements of capacitance C as a function of frequency and temperature show a decrease in C with increasing frequency and increase in C with increasing temperature. The increase in capacitance in the high-temperature low-frequency region is probably due to space charge polarization induced by the increasing number of free carriers as a result of increasing temperature.

M. Anwar (✉)
Physics Department, Government College, Burewala, Pakistan
e-mail: dr_anwar03@yahoo.com; dranwar03@brain.net.pk

I. M. Ghauri
Centre for Advanced Studies in Physics, G. C. University, Lahore, Pakistan

S. A. Siddiqi
Centre for Solid State Physics, University of the Punjab, Lahore, Pakistan

Introduction

Thin dielectric films are extensively used as capacitors in microelectronic devices. Charge transport measurements in disordered semiconductors and insulators have been of considerable interest recently because they can provide information about the electronic structure of these materials. The disorder in atomic configuration is thought to cause localized electronic states within the material.

Electrical conduction in metal oxides can take place by two parallel processes: (1) by free band conduction and (2) by hopping conduction in the localized states. The former tends to occur at higher temperatures, where carriers excited beyond the mobility edges into non-localized states, dominate the transport, while the latter may be due to carriers excited into localized state band edges [1], i.e.

$$\sigma = \sigma_i + \sigma_h \tag{1}$$

where σ_i is the intrinsic conductivity and σ_h the hopping conductivity. The intrinsic conductivity is expressed as

$$\sigma_i = \sigma_a \exp(E/kT) \tag{2}$$

where σ_a is constant, E is the thermal activation energy, k is the Boltzmann constant and T is the absolute temperature. The hopping conductivity is expressed as [1]

$$\sigma_h = \sigma_2 T^{1/2} \exp(-B/T^{1/4}) \tag{3}$$

where σ_2 and B are constants.

The a.c. conductivity, $\sigma_{a.c}$ in many amorphous solids has been found experimentally to obey an equation of the type [2]

$$\sigma_{a.c}(\omega, T) = A\omega^s \quad (4)$$

where ω is the angular frequency of the applied field, A is a complex proportionality constant and s is temperature-dependent parameter. The value of exponent s has been reported to be less than unity.

Different conduction mechanisms (hopping, tunnelling or free band) can lead to ω^s type of behaviour for a.c. conductivity. It is difficult to decide which of the mechanisms (hopping, tunnelling or free band) is responsible for the observed conduction properties. However, the behaviour of the exponent s with temperature can help elucidate various theories regarding Eq. 4.

Many authors have investigated the a.c. conduction mechanisms through thin insulating films and have explained their results in terms of different theoretical approaches [3, 4]. Shimakawa [5] proposed single polaron hopping (one electron hopping between a neutral defect, D^o, and a charged defect, D^+, and one hole between D^o and D^-) as well as bipolaron hopping (two electrons hopping between D^- and D^+ centres) to explain all the features observed in chalcogeuide glass semiconductors.

Materials exhibiting high optical transparency, electrical conductivity and efficient growth as thin films, are used extensively for a variety of applications including, thin film photovoltaics, optoelectronic devices, solar cells, ion-storage, flat panel displays, defrosting windows in refrigerators and airplanes and gas sensors [6–9]. Transparent conducting oxides, such as cadmium oxide, tin oxide, zinc oxide, indium tin oxide have great technological potential due to their right combination of electrical and optical properties [10]. Most of the well-known and widely used transparent conducting oxides thin films such as ZnO, SnO_2 and ITO are n-type material.

SnO_2 is a widely studied material in its thin film form due to various kinds of possible applications. Studies on the electrical and optical properties of SnO_2 thin films fabricated by various techniques such as chemical vapour deposition, sputtering, thermal evaporation, pyrosol and sol-gel dip coating technique have been reported by many workers [11–13]. Bulk stoichiometric SnO_2 is an insulator with a direct band gap of about 3.8 eV and an indirect band gap of about 2.7 eV [14]. Kim et al. [15] have reported that conduction band is mainly from tin 5s electrons and the valence band is from oxygen 2p electrons. The shapes of both conduction band and valence band are parabolic. High n-type conductivity in undoped SnO_2 is observed if it is oxygen deficient, since oxygen vacancies or interstitial Sn^{4+} ions are donor sites. The oxygen vacancies act as doubly ionized donors and contribute two electrons to the electrical conductivity [16].

The undoped SnO_2 is electrically conducting mainly as a result of deviation from stoichiometry. The n-type conductivity in non-stoichiometric SnO_2 is known to be due to interstitial tin atoms and oxygen vacancies. Carriers are formed by ionization of interstitial tin and oxygen vacancies [17].

A detailed investigation of electron energy structure of SnO_2 is of considerable theoretical and practical interest. Some researchers have reported results on various properties of SnO_2 [18–20], but no information about the a.c. conduction mechanisms in amorphous thin films of SnO_2 is available in literature. The study of a.c. electrical properties of evaporated amorphous thin films of SnO_2 helps to elucidate the basic properties of this oxide.

In this study we report the a.c. electrical properties of amorphous thin films of SnO_2. The structure and stoichiometry of the films are determined by the process parameters: namely film thickness, substrate temperature and post-deposition annealing. The effects of temperature on the conductivity–frequency and capacitance–frequency characteristics of the Al–SnO_2–Al structure are also reported.

Experimental work

Sample fabrication technique

Amorphous thin films used in this study were prepared by vacuum evaporation of high-purity SnO_2. This oxide was evaporated from an electrically heated molybdenum boat in a Balzers BA 510 coating unit. The oxide was deposited at a pressure of 1.33×10^{-4} Pa without any gas treatment. Films in the thickness range 100–400 nm were deposited at a rate of 0.75 nms^{-1} with the substrates at 293 K. Some 300 nm-thick samples were fabricated with substrates in the temperature range 293–543 K. Al–SnO_2–Al samples were prepared on clean Corning 7059 glass substrate by the sequential vacuum deposition of aluminium as the bottom electrode, SnO_2 as the insulator and aluminium as the top electrode in a crosswise fashion having width $\approx$3 mm so that the film capacitor has an effective area of 0.1 cm^2 approximately. Aluminium electrodes were made sufficiently thick so that their resistance was less than 2–3 Ω. The substrates were heated to the required temperature by the heater mounted at the inner top of the bell jar. The thickness of the film was estimated using a quartz crystal monitor and finally the exact film thickness was determined by multiple beam interferometry (MBI). Some samples were annealed in vacuum for 4 h at different temperatures and allowed to cool down at the rate of 2 K/min.

A number of films were deposited and for convenience only those films whose respective thickness was in exact

number such as 100, 200, 300 nm etc. were selected for electrical measurements The thickness was measured very carefully by MBI; however, the chance of error in the measurement is only approximately ±2–3 nm in each sample. The samples were heated in a subsidiary vacuum system to remove absorbed gaseous impurities prior to electrical measurements. All other techniques used for fabrication of samples and cleaning the glass substrates are the same as described earlier by Anwar et al. [21].

A.c. measurements

A.c. electrical measurements were made by a conventional method with the sample in a subsidiary vacuum system at a pressure of the order of 1.33×10^{-4} Pa. The lowering of the sample temperature was achieved by firmly attaching the sample to the brass base of a stainless steel tank containing liquid nitrogen. Heating the sample above room temperature was initiated by using a resistance heater inserted in the holes made through the brass base. A chromel–alumel thermocouple was attached to the substrate close to the metal–insulator–metal (MIM) capacitor under test, so as to measure the device temperature accurately. Silver paste was used to make good electrical and thermal contacts. A.c. measurements were taken directly using a Hewlett-Packard Impedance Analyser type L. F. 4192 A, for conductance, capacitance and Q factor (quality factor) of the sample, in the frequency range 300–1 MHz using an a.c. signal of 500 mV applied across each sample. The relative dielectric constant ε_r, was calculated from the well-known expression $C = \varepsilon_r \varepsilon_o A/d$ where A is the active area of the device, d—the thickness of the film, C the capacitance of the film capacitor and ε_o is the permittivity of free space. The area of the film capacitor was determined by a simple travelling microscope.

Results

The a.c. conduction mechanisms of high-quality thermally evaporated amorphous thin films of SnO_2 have been studied as a function of film thickness, substrate temperature and post-deposition annealing. The variation in a.c conductivity with frequency at different temperatures in the range 193–393 K for a 300 nm-thick Al–SnO_2–Al sandwich sample deposited on the substrate kept at 293 K is shown in Fig. 1. This type of frequency variation of a.c. conductivity component, $\sigma_{a.c}$, is expressed by the relation $\sigma_{a.c} = A\omega^s$ (Eq. 4). The values of index s were obtained by evaluating the slope of logσ versus log$f$ curves of Fig. 1, which ranges from 0.62 to 0.93. Four Al–SnO_2–Al sandwich samples deposited on the substrates kept at 293 K having film thicknesses in the range 100–400 nm were studied at 293 K

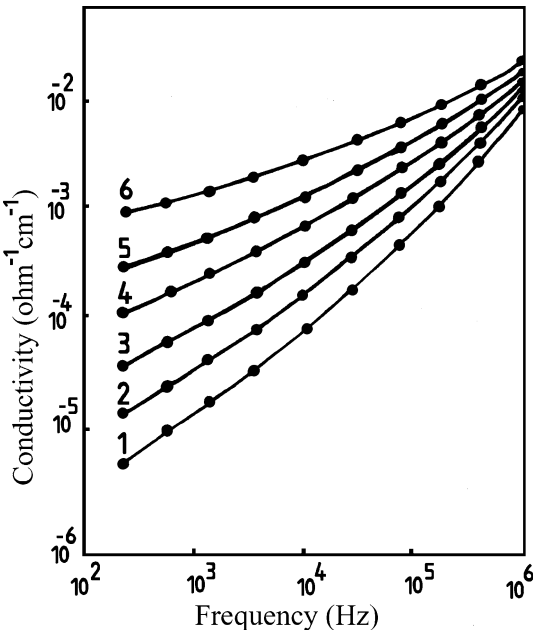

Fig. 1 Variation of a.c. conductivity with frequency of 300 nm-thick Al–SnO_2–Al sample at various temperatures during electrical measurements, (1) 193 K, (2) 233 K, (3) 273 K, (4) 313 K, (5) 353 K, (6) 393 K

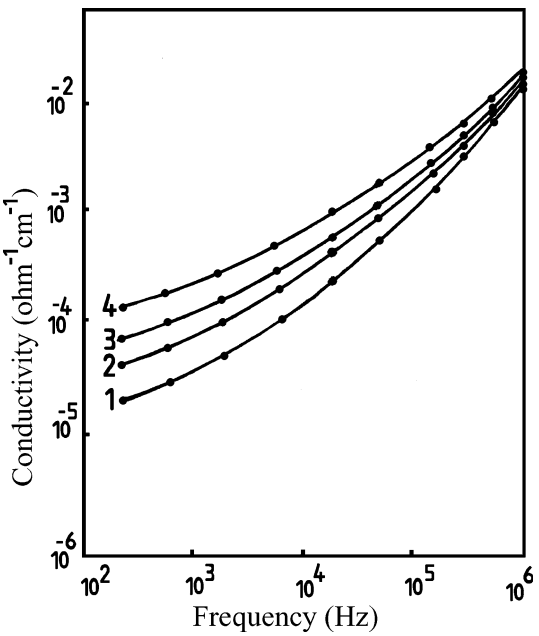

Fig. 2 Variation of a.c. conductivity with frequency of Al–SnO_2–Al samples at various thicknesses, (1) 100 nm, (2) 200 nm, (3) 300 nm, (4) 400 nm

(during measurements in a subsidiary vacuum system) and their frequency–conductivity characteristics are shown in Fig. 2. Four 300 nm-thick Al–SnO_2–Al sandwich samples deposited in the substrate temperature range 293–543 K were studied at 293 K (during measurements in a subsidiary vacuum system) and their frequency–conductivity

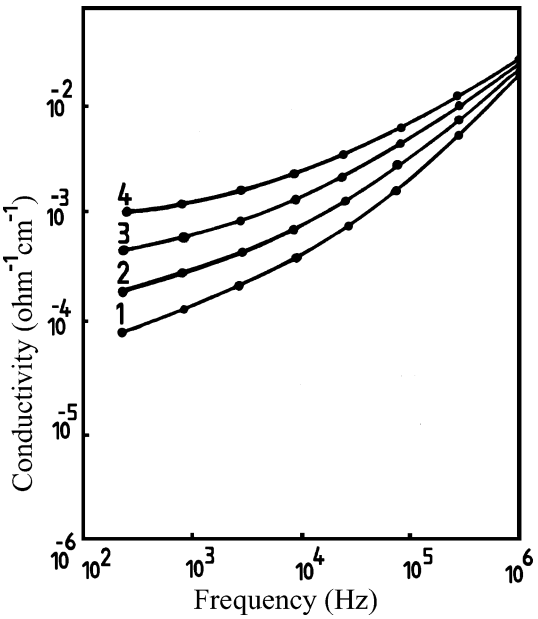

Fig. 3 Variation of a.c. conductivity with frequency of 300 nm-thick Al–SnO_2–Al samples at various substrate temperatures, (1) 293 K, (2) 373 K, (3) 473 K, (4) 543 K

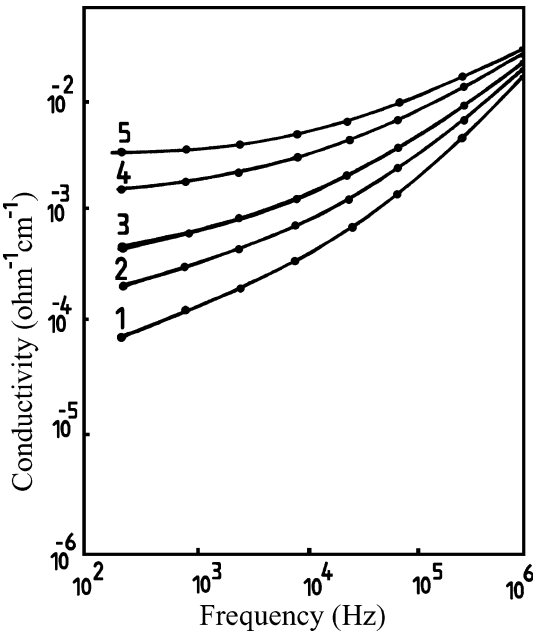

Fig. 4 Variation of a.c. conductivity with frequency of 300 nm-thick Al–SnO_2–Al samples at various annealing temperatures, (1) as evaporated, (2) 473 K, (3) 573 K, (4) 673 K, (5) 773 K

characteristics are shown in Fig. 3. Five 300 nm-thick Al–SnO_2–Al sandwich samples deposited at substrate temperature 293 K and annealed in the temperature range 473–773 K were studied at 293 K (during measurements in a subsidiary vacuum system) and their frequency–conductivity characteristics are shown in Fig. 4. The a.c. conduction process follows an ω^s-type law with s decreasing with increase in temperature. The graphs drawn in Figs. 1–4 are not linear but there is a small curvature in these plots. Results presented in these plots are similar to those as reported by other authors [22–25]. For higher frequency the conductivity approaches a quadratic power law. Figure 5 shows the variation of a.c conductivity with the inverse of temperature at different frequencies for the sample of Fig. 1. The essential feature in the temperature and frequency dependence of a.c conductivity is that at low temperature the conductivity is strongly frequency dependent. The values of activation energies estimated from the slope of these plots are given in Table 1. It was observed that at higher temperatures the direct current (d.c.) part of conductivity approaches the a.c conductivity value. It is worth noting that at higher frequencies the activation energy has much smaller values, indicating a different conduction process at higher frequencies. These values are consistent with the existence of a hopping mechanism in the lower temperature region and thermally activated free band conduction process at higher temperature region.

The dependence of slope s of σ–f curves for the sample of Fig. 1 as a function of temperature T is shown in Fig. 6, which maybe expressed as [26]

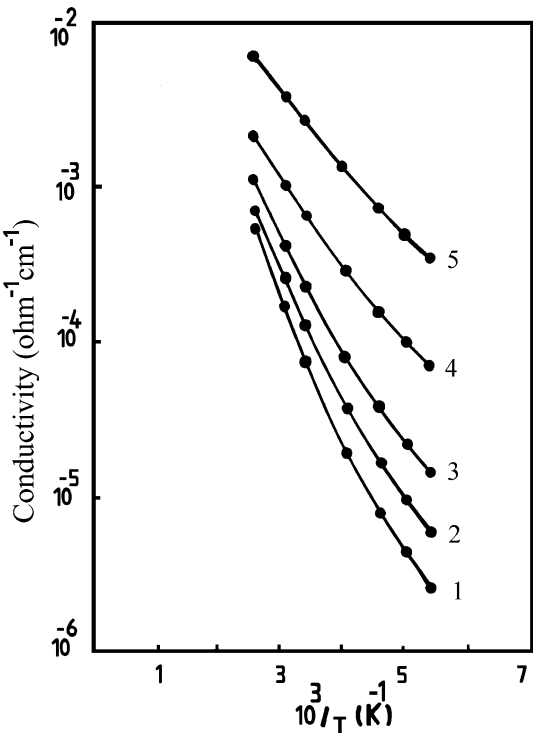

Fig. 5 Conductivity plotted as a function of 1000/T for a 300 nm-thick Al–SnO_2–Al sample of Fig. 1, for fixed frequencies (1) d.c. (at 0.2 V), (2) 0.3 kHz, (3) 1 kHz, (4) 10 kHz, (5) 100 kHz

$$s = \mathrm{d}\log\sigma/\mathrm{d}\log f = -AT + B \tag{5}$$

where A and B are positive constants, f the frequency ($\omega/2\pi$) and T the absolute temperature. Hence $\sigma_{ac} = f^{-(AT - B)}$

Table 1 Activation energy for two ranges of temperature of a 300 nm-thick Al−SnO_2−Al sample at various applied frequencies

Frequency (kHz)	Activation energy (eV)	
	193−230 K	345−393 K
0 d.c. (at 0.2 V)	0.062	0.45
0.3	0.050	0.40
1.0	0.047	0.35
10	0.042	0.31
100	0.020	0.22

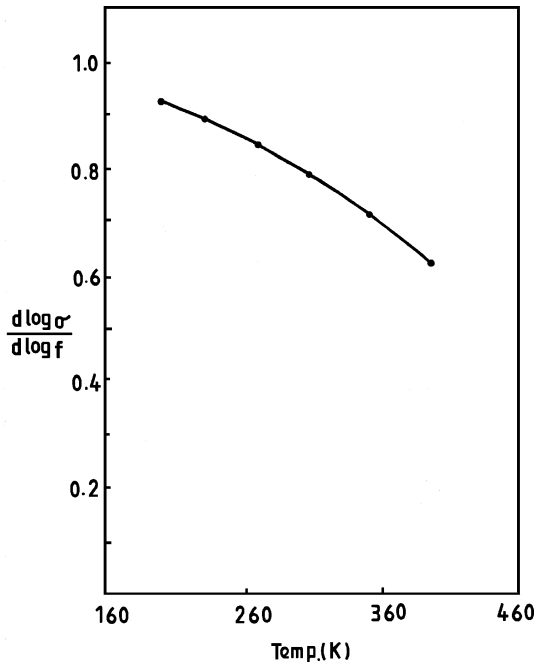

Fig. 6 Temperature dependence of the slope of conductivity–frequency characteristics as a function of temperature for the sample of Fig. 1

gives the effect of simultaneous variation of temperature and frequency on a.c. conductivity. It is seen from Fig. 6 that the value of s decreases from 0.93 to 0.62 when the temperature increases from 193 to 393 K.

Theoretically, the total conductivity $\sigma(\omega)$ measured in a.c. fields for semiconductors or insulators can be written as

$$\sigma(\omega) = \sigma_{dc} + \sigma_{ac} \tag{6}$$

where σ_{dc} is the direct current (d.c.) conductivity and σ_{ac} is the component of conductivity depending upon the frequency of the applied field.

Figure 7 shows the variation of capacitance with frequency of a 300 nm-thick Al–SnO_2–Al sandwich sample at various temperatures during electrical measurements. A decrease of capacitance with increasing frequency is noted and this is probably associated with an increase in current leakage with increase in frequency, a phenomenon that is

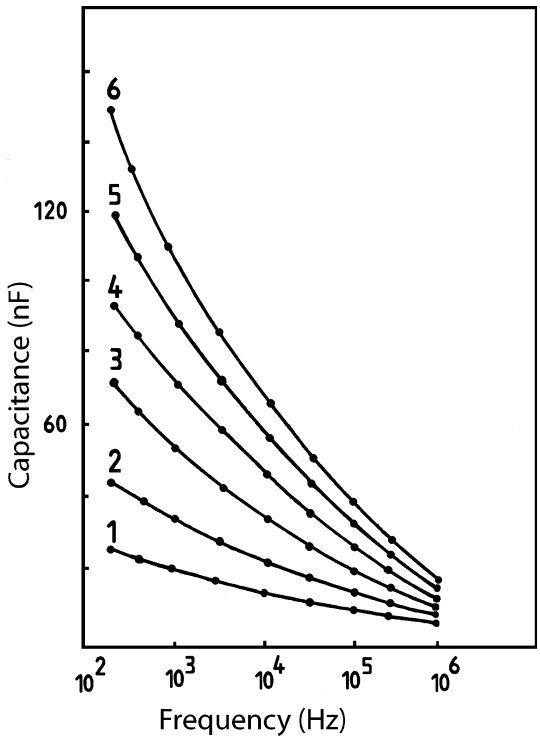

Fig. 7 Variation of capacitance with frequency of a 300 nm-thick Al–SnO_2–Al sample at various temperatures during electrical measurements, (1) 193 K, (2) 233 K, (3) 273 K, (4) 313 K, (5) 353 K, (6) 393 K

normally associated with a capacitance reduction. The change in capacitance with frequency becomes less remarked as the temperature is decreased. The variation of capacitance C, with frequency f, below 10^4 Hz for the temperature range 193–393 K is of the form

$$C \propto f^{-1/x} \tag{7}$$

where x is approximately equal to 6 [27].

Discussion

To analyse the present results, different existing theories for the a.c. conductivity related to ω^s behaviour will be considered and a reasonable model, which explains the a.c behaviour of SnO_2, will be suggested. Figure 5 shows the graph between conductivity versus reciprocal temperature. The slope of this graph yields the activation energy. To interpret the present results we first of all apply a model initially proposed by Pollak and Geballe [28]. According to this model thermally assisted hopping conduction mechanism is involved between localized states. They further suggested that at higher temperature multiple hops occur frequently, while at low temperature a single hop predominates. This leads to an increased thermal activation at high temperatures with a corresponding decrease in

frequency dependence. But in our results conductivity shows strong frequency dependence, which is coupled with low-activation energy at low temperature (Table 1). Thus present results cannot be explained on the basis of Pollak and Geballe [28] theory.

Austin and Mott [3] improved the theory of Pollak and Geballe and assumed that a.c. conduction process takes place by the hopping of electrons between pairs of localized states at the Fermi level. This process can be imagined as a phonon-assisted tunnelling process through the potential barrier between the localized states. Austin and Mott [3] have given the following expression for the a.c. conductivity

$$\sigma_{a.c}(\omega) \propto (\pi/3)[N(E_F)^2]kTe^2\alpha^{-5}\omega[\ln(\upsilon_{ph}/\omega)]^4 \quad (8)$$

where υ_{ph} is the phonon frequency and α is the exponential decay parameter of localized states wave functions. Equation 8 shows that a.c conductivity is directly proportional to the absolute temperature but in our case $\sigma_{a.c}$ is not directly proportional to the absolute temperature.

Austin and Mott [3] further suggested that to consider the effect of polaron formation the last term in Eq. 8 must be replaced by $[\ln(\upsilon_{ph}/\omega) - W_H/kT]^4$, where W_H is the polaron hopping energy. The mathematical expression for conductivity takes the form:

$$\sigma_{a.c}(\omega) \propto (\pi/3)[N(E_F)^2]kTe^2\alpha^{-5}\omega[\ln(\upsilon_{ph}/\omega) - W_H/kT]^4 \quad (9)$$

The exponent s for the frequency power law behaviour of the conductivity at high frequencies is given by the expression:

$$s = d[\ln\sigma_{ac}(\omega)]/d(\ln\omega) = 1 - 4/\ln(\upsilon_{ph}/\omega) \quad (10)$$

Equation 10 shows that s is a decreasing function of frequency. When last term in Eq. 10 is replaced by $[\ln(\upsilon_{ph}/\omega) - W_H/kT]$, the value of s becomes temperature dependent and can be written as

$$s = \{1 - 4/[\ln(\upsilon_{ph}/\omega) - W_H/kT]\} \quad (11)$$

and the variation of s with temperature is given by the expression:

$$ds/dT = 4W_H/\left\{kT^2\left[\ln(\upsilon_{ph}/\omega) - W_H/kT\right]^2\right\} \quad (12)$$

Equation 12 shows that ds/dT is always positive so s increases with increase in temperature, but in our case a decrease in s is observed with increase in temperature. Thus from Eqs. 8 and 12, it is concluded that the theory of Austin and Mott is unable to explain the a.c behaviour of SnO_2.

Elliott [2] proposed a correlated hopping model to account for the a.c. conductivity in amorphous materials. This model is based on the hopping of charge carriers between localized sites separated by barriers of height W_m, identified with the optical band gap. According to this model a.c. conductivity is given by the expression:

$$\sigma(\omega) = \left(\pi^2N^2\varepsilon/24\right)\left(8e^2/\varepsilon W_m\right)^6\left(\omega^s/\tau_o^\beta\right) \quad (13)$$

where N is the density (concentration) of localized states, $s = 1 - \beta$ at low temperature, $\beta = 6kT/W_m$, W_m is the value of optical band gap and τ_o is the characteristic relaxation time ($\approx 10^{-13}$ s). Equation 13 predicts a frequency response of conductivity proportional to ω^s, with s increasing and tending to unity as temperature is decreased. In the present case a gradual increase in s is observed with decrease in temperature and conductivity is strongly frequency dependent. At high frequency and low temperature the activation energy is low (0.02 eV). These features indicate that conduction at high frequency and low temperature is by hopping mechanism.

The pair relaxation time is assumed to be

$$\tau = \tau_o\exp(W/kT) \quad (14)$$

The exponent s is related to W_m by

$$s = 1 - 6kT/W_m \quad (15)$$

By putting the measured value of optical band gap (2.78 eV) [29] of 300 nm-thick sample of SnO_2 deposited at 293 K in Eq. 15, the value of s is found out to be 0.95 at room temperature, which is consistent with the measured value (0.93), as derived from the data of Fig. 1 at a frequency of $\approx 10^5$ Hz. As the theoretical value of $s = 0.95$ calculated from Eq. 15 agrees with the experimental value of 0.93, we conclude that the conduction mechanism in our films is governed by Elliott [2] theory of single polaron hopping.

Thus the Elliott model satisfactorily explains the temperature and frequency dependence of a.c conductivity and variation of exponent s with temperature, which suggests that electron-hopping process dominates at lower temperature region and thermally activated free band conduction process dominates at higher temperature region. The transition from hopping to free band conduction is due to overlapping of localized levels and the free band. These results are consistent with those of other authors [22–26, 30–32].

The observed results are explained as follows:

It is observed that a.c. conductivity increases due to increase in temperature during measurements of electrical properties of the sample. The thermal evaporation of SnO_2 in vacuum produces lattice oxygen vacancies, which are responsible for electron production in thin films. Oxygen vacancies are shallow defects whose ionization occurs easily. Ionized oxygen vacancy provides carriers for conduction. At higher temperature oxygen vacancies act as doubly ionized donors and contribute two electrons as

charge carriers. The increase in conductivity due to increase in temperature during measurements of electrical properties of the sample is likely due to increase in the formation and high mobility of these types of ionized donors.

The thickness is one of the most important parameters, which affects the electrical properties of amorphous thin films. It has been observed that electrical conductivity is increased with the increase in film thickness of SnO_2. The carriers are formed due to the interstitial tin, oxygen vacancies and defects produced due to deviation from stoichiometry during evaporation [i.e. Sn_2O_i (where O_i is the interstitial oxygen bound to tin), Sn_2O_4 and SnO_{2-x} $(V_{\ddot{o}})_x$ e'_{2x} defects (where x is the deviation from stoichiometry)], but the mechanism responsible for large semi-conducting changes in SnO_2 thin films is the formation of oxygen vacancies [18]. The oxygen vacancies drastically alter the electronic properties of thin films making hopping of electrons between the oxygen vacancies. When the thickness of amorphous thin films is increased the concentration of oxygen vacancies is increased. An oxygen vacancy is formed when an oxygen atom in a normal lattice site is removed, which is usually equivalent to a transformation of an oxygen atom in a normal site to the gaseous state. Considering that oxygen ions in the regular sites have a valency of -2, in this process, the two electrons of the oxygen ion are left in the vacant site. If one or both of the localized electrons are excited and transferred away from the vacancy, the oxygen vacancy becomes singly or doubly ionized, respectively. Since electrons are removed, the ionized oxygen vacancy will have an effective positive charge to conserve the electrical neutrality of the material. The charged vacancy becomes an electron-trapping site but in this process one or two electrons are available for conduction. The formation of charged oxygen vacancy leads to the formation of complimentary free electrons. Thus initially when the thickness is increased, interstitial tin, oxygen vacancies and Sn_2O_i, Sn_2O_4 and SnO_{2-x} $(V_{\ddot{o}})_x$ e'_{2x} defects generate carriers in the films. Oxygen vacancies, interstitial tin and defects produced due to deviation from stoichiometry are donor like. A large concentration of donor centres effectively increases the conductivity in thicker samples.

The main conduction mechanism in SnO_2 thin films deposited at higher substrate temperature is the creation of oxygen vacancies. During increase in substrate temperature a large increase in the free electron concentration occurs due to increase in the number of charged oxygen vacancies. When an oxygen vacancy is initially formed at higher substrate temperature, the chemical bonds of an oxygen atom to the neighbouring atoms are broken. Therefore, it is expected that process of formation of oxygen vacancy is related to the oxygen bond strength in the tin oxide. From this point of view, tin oxide is considered a relatively unstable material, so that it is relatively easy to be reduced from higher to lower valence states. Thus increase in conductivity due to increase in substrate temperature is ascribed to the oxygen vacancies and formation of tin species of lower oxidation states.

It has been observed that electrical conductivity is increased with the increase in annealing temperature. In SnO_2 singly and doubly ionized oxygen vacancies are thought responsible for semiconducting properties at higher annealing temperature. When SnO_2 is annealed in vacuum, singly ionized oxygen vacancy is changed into doubly ionized oxygen vacancy, and small number of Sn^{4+} ions is changed into Sn^{2+} ions. Thus the formation of tin species of lower valence states and doubly ionized oxygen vacancies are thought responsible for increase in electrical conductivity at higher annealing temperature.

The capacitance is observed to decrease with the rise in frequency as shown in Fig. 7. This decrease in capacitance with frequency becomes less prominent for lower temperatures. As temperature increases the low-frequency range capacitance increases markedly. The increase in capacitance in the high-temperature low-frequency region is probably due to space charge polarization induced by the increasing number of free carriers as a result of increasing temperature. Such dispersion in the capacitance has been attributed to the non-stoichiometric nature of the films.

The capacitance characteristics described above are similar to those observed by Goswami and Goswami [27]. The general variations of capacitance with both frequency and temperature can be explained by using the equivalent circuit model proposed by these workers, which consists of a fixed capacitive element C in parallel with a resistive element R, together with a series lead resistance r. The model assumes that the contacts are ohmic and do not form Schottky barriers at the surface. The measured series equivalent capacitance C_s, is given by [27]

$$C_s = C + 1/\omega^2 R^2 C \tag{16}$$

where C is a frequency independent capacitance and R is assumed to be thermally activated and is given by [27]

$$R = R_0 \exp(\Delta E/kT) \tag{17}$$

where R_0 is a constant and ΔE is activation energy. From Eq. 17, it is clear that increase in the value of temperature implies a decrease of R and hence measured capacitance increases with the increase of temperature (using Eq. 16). Equation 16 also predicts that measured capacitance should decrease with increasing frequency reaching a value of $C_s = C$ for $f = \infty$ Hz. This effect is confirmed in the C versus f plot shown in Fig. 7.

Conclusion

On the basis of above-mentioned observations, it is concluded that the a.c. conduction mechanism in our films is governed by Elliott theory of single polaron hopping which suggests that electron-hopping process dominates at lower temperature region and thermally activated free band conduction process dominates at higher temperature region. The transition from hopping to free band conduction is due to overlapping of localized levels and the free band. The increase in electrical conductivity with increase in temperature during electrical measurements is ascribed to the increase in the formation and high mobility of doubly ionized oxygen vacancies. The increase in conductivity with increase in film thickness is caused by the increase in interstitial tin, oxygen vacancies and defects produced due to deviation from stoichiometry. The increase in conductivity with increase in substrate and annealing temperature may be due to the formation of singly or doubly ionized oxygen vacancies and tin species of lower oxidation state. Measurements of capacitance C as a function of frequency and temperature show a decrease in C with increasing frequency and increase in C with increasing temperature. The increase in capacitance in the high-temperature low-frequency region is probably due to space charge polarization induced by the increasing number of free carriers as a result of increasing temperature.

References

1. Mott NF (1972) J Non-Cryst Solids 1:1. doi:10.1016/0022-3093(68)90002-1
2. Elliott SR (1978) Philos Mag B 37:553. doi:10.1080/01418637808226448
3. Austin IG, Mott NF (1969) Adv Phys 18:14. doi:10.1080/00018736900101267
4. Pollak M (1971) Philos Mag 23:519. doi:10.1080/14786437108216402
5. Shimakawa K (1982) Philos Mag B 46:123. doi:10.1080/13642818208246429
6. Omura K, Veluchamy P, Tsuji M, Nishio T, Murojono D (1999) J Electrochem Soc 146:2113. doi:10.1149/1.1391900
7. Laverty SJ, Feng H, Maguire P (1997) J Electrochem Soc 144:2165. doi:10.1149/1.1837758
8. Tadeev AV, Delabouglise G, Labeau M (1998) Mater Sci Eng B 57:76
9. Ahmed SKF, Khan S, Ghosh PK, Mitra MK, Chattopadhyay KK (2006) J Sol-Gel Sci Technol 39:241. doi:10.1007/s10971-006-7808-x
10. Suh S, Zhang Z, Chu WK, Hoffman DM (1999) Thin Solid Films 345:240. doi:10.1016/S0040-6090(98)01421-7
11. Cachet H, Gamard A, Campet G, Jousseaume B, Toupance T (2001) Thin Solid Films 388:41
12. Mohagheghi MMB, Saremi MS (2004) J Phys D Appl Phys 37:1248. doi:10.1088/0022-3727/37/8/014
13. Ji Z, He Z, Song Y, Liu K, Xiang Y (2004) Thin Solid Films 460:324. doi:10.1016/j.tsf.2004.02.021
14. Morais EA, Scalvi LVA, Geraldo V, Scalvi RMF, Ribeiro SJL, Santilli CV et al (2004) J Eur Ceram Soc 24:1857
15. Kim H, Gilmore CM, Pique A, Horwitz JS, Mattoussi H, Murata H, Kafafi ZH, Chrisey DB (1999) J Appl Phys 86:6451. doi:10.1063/1.371708
16. Rockenberger J, Felde UZ, Tischer M, Troger L, Haase M, Weller H (2000) J Chem Phys 112:4296. doi:10.1063/1.480975
17. Banerjee AN, Maity R, Kundoo S, Chattopadhyay KK (2004) Phys Status Solidi (a) 201(5):983. doi:10.1002/pssa.200306766
18. Tahar RBH, Ban T, Ohya Y, Takahashi Y (1997) J Appl Phys 83(5):2631. doi:10.1063/1.367025
19. Karapatnitski IA, Mit KA, Mukhamedshina DM, Beisenkhanov NB (2002) Surf Coat Technol 151–152:76. doi:10.1016/S0257-8972(01)01611-5
20. Lee JS, Choi SC (2005) J Eur Ceram Soc 25:3307. doi:10.1016/j.jeurceramsoc.2004.08.022
21. Anwar M, Ghauri IM, Siddiqi SA (2005) Czech J Phys 55(8):1013. doi:10.1007/s10582-005-0100-4
22. Anthopoulos TD, Shafai TS (2003) J Appl Phys 94(4):2426. doi:10.1063/1.1592626
23. El-Nahass MM, El-Barry AMA, Rahman SA (2006) Phys Status Solidi (a) 203(2):317. doi:10.1002/pssa.200521304
24. Kitaneh RML, Saleh AM, Gould RD (2006) Cent Eur Sci J 4(1):87. doi:10.1007/s11534-005-0008-4
25. Mahmood FS, Gould RD (1994) Thin Solid Films 253:529. doi:10.1016/0040-6090(94)90379-4
26. Ismail BB, Gould RD (1996) Proc SPIE 2780:46. doi:10.1117/12.238200
27. Goswami A, Goswami AP (1973) Thin Solid Films 16:175. doi:10.1016/0040-6090(73)90166-1
28. Pollak M, Geballe TH (1961) Phys Rev 122:1742. doi:10.1103/PhysRev.122.1742
29. Anwar M, Ghauri IM, Siddiqi SA (2007) Int J Mod Phys B 21(12):2017
30. El-Wahabb EA (2005) Acta Phys Pol A 108(6):985
31. Amma DSD, Vaidyan VK, Manoj PK (2005) Mater Chem Phys 93:194
32. Jarzebski ZM (1982) Phys Status Solidi (a) 71:13. doi:10.1002/pssa.2210710102